Available online at www.sciencedirect.com
ScienceDirect
Ultramicroscopy 108 (2008) 167–178
ultramicroscopy
www.elsevier.com/locate/ultramic

Prerequisites for a C_c/C_s-corrected ultrahigh-resolution TEM

M. Haider[a,*], H. Müller[a], S. Uhlemann[a], J. Zach[a], U. Loebau[a], R. Hoeschen[b]

[a]CEOS GmbH, Englerstr. 28, D-69126 Heidelberg, Germany
[b]Max Planck Institut für Metallforschung, Heisenbergstraße 3, D-70569 Stuttgart, Germany

Abstract

After the introduction of a corrector to compensate for the spherical aberration of a TEM and the acceptance of this new instrumentation for high-resolution CTEM (conventional transmission electron microscope) and STEM (scanning transmission electron microscope) by the electron microscopy community, a demand for even higher resolution far below 1 Å has emerged. As a consequence several projects around the world have been launched to make these new instruments available and to further push the resolution limits down toward fractions of 1 Å. For this purpose the so-called TEAM (transmission electron aberration-corrected microscope) has been initiated and is currently under development.

With the present paper we give a detailed assessment of the stability required for the base instrument and the electric stability, the manufacturing precision, and feasible semi-automatic alignment procedures for a novel C_c/C_s-corrector in order to achieve aberration-free imaging with an information limit of 0.5 Å at an acceleration voltage of 200 kV according to the goals for the first TEAM instrument. This new aberration corrector, a so-called Achroplanat, in combination with a very stable high-resolution TEM leads to an imaging device with unprecedented resolving power and imaging properties.
© 2007 Elsevier B.V. All rights reserved.

PACS: 41.85.−p; 41.85.Gy; 87.64.Ee; 87.61.Ff

Keywords: High-resolution TEM; Electron microscope design; Particle optics; Aberration correction

1. Introduction

Already 70 years ago Scherzer [1] proved the impossibility to correct for the spherical and the chromatic aberrations of a charged particle lens just by a combination of ordinary lenses as it can be achieved for light-optical instruments. His fundamental finding is nowadays called the Scherzer theorem. Scherzer not only stated the problem but he also gave a theoretical survey of possible solutions [2]. By taking his theorem into account it is clear which techniques can be used to compensate for either one or both primary aberrations. One has to break one of the postulates that the electromagnetic focusing fields are free of space charge, time-independent and cylinder-symmetric and the optic axis has no point of reversal. Breaking the cylindrical symmetry for the fields or employing a reflecting device are currently the methods of choice. During the last decade multipole correctors and mirror correctors have been realized successfully to correct for C_c and/or C_s of various charged particle lenses [3,4].

Beside multipole and mirror correctors there are two additional possibilities for the correction of aberrations. However, up to now it does not seem to be realistic to mount a charge in vacuum which, on one hand does not cause scattering but on the other hand introduces forces which could compensate deviations from the ideal ray path due to the spherical and/or chromatic aberration. The second theoretically feasible method for the correction of axial aberrations is the application of time-varying fields which would need a pulsed electron source and very high-frequency electromagnetic fields. For modern microscopes used nowadays one would need frequencies in the range of GHz for accelerating voltages in the range of 200 kV.

The hexapole-type C_s-correctors for the conventional transmission electron microscope (CTEM) [5,6] and the

*Corresponding author.
E-mail address: haider@ceos-gmbh.de (M. Haider).

0304-3991/$ - see front matter © 2007 Elsevier B.V. All rights reserved.
doi:10.1016/j.ultramic.2007.07.007

Table 1
List of the upper limits with respect to the $\pi/4$ criterion of all axial aberrations considering only one particular aberration coefficient

Aberration	80 kV	120 kV	200 kV		300 kV
	80 pm	65 pm	100 pm	50 pm	50 pm
Focus C_1 (nm)	0.40	0.31	1.0	0.25	0.4
Two-fold astigmatism A_1 (nm)	0.40	0.31	1.0	0.25	0.4
Three-fold astigmatism A_2 (nm)	11.50	9.2	60.0	7.5	13
Second-order coma B_2 (nm)	3.80	3.1	20.0	2.5	5.0
Third-order spherical aberr. C_3 (μm)	0.30	0.24	3.2	0.2	0.5
Four-fold astigmatism A_3 (μm)	0.30	0.24	3.2	0.2	0.5
Third-order star aberr. S_3 (μm)	0.07	0.06	0.8	0.05	0.11
Five-fold astigmatism A_4 (μm)	8.2	6.4	16.0	5.0	13.
Fourth-order coma B_4 (μm)	1.65	1.3	3.2	1.0	2.6
Fourth-order three-lobe aberr. D_4 (μm)	1.65	1.3	3.2	1.0	2.6
Fifth-order spher. aberr. C_5 (mm)	0.17	0.13	7.68	0.12	0.4
Six-fold astigmatism A_5 (mm)	0.17	0.13	7.68	0.12	0.4
Fifth-order rosette aberr. R_5 (mm)	0.03	0.02	1.28	0.02	0.06
Fifth-order star aberr. S_5 (mm)	0.03	0.02	1.28	0.02	0.06
Seven-fold astigmatism A_6 (mm)	4.58	3.62	358.4	2.8	11.7
Sixth-order coma B_6 (mm)	0.65	0.52	51.2	0.4	1.7
Sixth-order three-lobe aberr. D_6 (mm)	0.65	0.52	51.2	0.4	1.7
Sixth-order pentacle aberr. F_6 (mm)	0.65	0.52	51.2	0.4	1.7
Seventh-order spher. aberr. C_7 (mm)	104	82.0	15904	62.2	339
Chromatic aberr. C_{c1} (μm)	10.	10.	10.	10.	10.

The summation of the total phase shift when all aberrations are contributing to the upper limit is not included.

scanning transmission electron microscope (STEM) already could demonstrate their advantages by various applications [7–9]. After this success the second important axial aberration, the chromatic aberration, remains to be compensated by an appropriate correction system.

For the purpose of an improvement of the resolving power of a TEM, not only the correction of the chromatic aberration has to be considered but in almost the same manner the requirements on the base instrument have to be investigated. The careful setup of the base instrument is as important as the correction system because, as it has already been stated several times: A correction system, even if it is the most advanced system, cannot compensate for incoherent parasitic aberrations of the base instrument caused, for example, by instabilities of power supplies or any mechanical component.

Hence, we will investigate the requirements for the complete system and define prerequisites for both parts: the correction system as well as the base instrument. Budgets of acceptable noise levels for the various components will be specified and must be met by all components in order to achieve finally a certain contrast at the required spatial frequency.

2. Aberration-free imaging

An aberration-free imaging (AFI) system does not exist. Every charged particle lens has intrinsic aberrations and in addition, an electron optical system can never be constructed with the mechanical precision required for perfect alignment. Therefore, at least residual parasitic aberrations are always present in real systems due to manufacturing tolerances of the optical elements and misalignments. If one demands for so-called "aberration-free imaging" one first has to define the limits within which "aberration-free imaging" has to be achieved.

2.1. Axial aberrations

Coherent or geometrical aberrations cause a residual phase shift of the electron wave leading to a directly observable displacement of the electron trajectories from the ideal shape of a non-aberrated beam.

The phase shift $\Delta\Phi(g)$ is related to the Eikonal function of the imaging system by

$$\phi(g) = 2\frac{\pi}{\lambda}\chi(\omega) \tag{1}$$

with the scattering vector g, the complex-valued scattering angle $\omega = \lambda g$, and the wavelength λ. The Eikonal function with all axial geometrical aberrations up to Seidel orders $n \leqslant 7$ has the following form:

$$\chi(\omega) = \mathrm{Re}\left\{\begin{array}{c} \tfrac{1}{2}\omega\varpi C_1 + \tfrac{1}{2}\varpi^2 A_1 + \tfrac{1}{3}\varpi^3 A_2 + \omega^2\varpi B_2 \\ +\tfrac{1}{4}(\omega\varpi)^2 C_3 + \tfrac{1}{4}\varpi^4 A_3 + \omega^3\varpi S_3 + \tfrac{1}{5}\varpi^5 A_4 \\ +\omega^3\varpi^2 B_4 + \omega^4\varpi D_4 + \tfrac{1}{6}(\omega\varpi)^3 C_5 + \tfrac{1}{6}\varpi^6 A_5 \\ +\omega^5\varpi R_5 + \omega^4\varpi^2 S_5 + \tfrac{1}{7}\varpi^7 A_6 + \omega^4\varpi^3 B_6 \\ +\omega^5\varpi^2 D_6 + \omega^6\varpi F_6 + \tfrac{1}{8}(\omega\varpi)^4 C_7 \\ +\tfrac{1}{8}\varpi^8 A_7 + \omega^7\varpi G_7 + \omega^6\varpi^2 R_7 + \omega^5\varpi^3 S_7 \end{array}\right\}. \tag{2}$$

The various aberrations up to the seventh order are listed in Table 1. To achieve good optical properties the residual

phase shift for electrons scattered in large aperture angles must be kept small. The classical criterion is to keep the maximum phase shift across the aperture introduced by a single dominant aberration below $|\Delta\Phi| \leqslant \pi/4$. This requirement becomes somewhat questionable if in an aberration-corrected system the one and only dominant aberration does not exist but a larger set of small aberrations acts together. Nevertheless, in Table 1 the upper limits of the axial aberrations with respect to a residual phase shift of $|\Delta\Phi| \leqslant \pi/4$ are listed in order to give an impression of the various values of the aberrations one can accept. The $\pi/4$-criterion for AFI is on one hand very strict. On the other hand for precise measurements of phase shifts by real objects, for example in electron holography, the requirements are even higher and the maximum residual phase shift by the aberrations should be below $|\Delta\Phi| \leqslant \pi/8$ [10].

Since aberrations having the same multiplicity can partially compensate each other, a reasonable generalization of the classical criterion is to make the maximum phase shift relative to the zero beam across the aperture for each set of aberrations with unique multiplicity smaller than $|\Delta\Phi| \leqslant \pi/4$. For a C_c/C_s-corrector the aberration of first to fourth (or even fifth) order can be tuned independently. Hence, these aberrations can be adjusted such that disturbing higher-order aberrations are optimally counter-balanced across the usable aperture. Alignment tools (ATs) or "generalized stigmators" will be available to tune the lower-order aberrations with a granularity much better than their individual $\pi/4$-effect. This procedure additionally requires that the residual phase shift can be measured with a precision better than $\pi/4$.

We consider different multiplicities separately. For each multiplicity one can derive an inequality for the residual aberrations, and these inequalities are called the AFI limits. An alternative and slightly harder measure would be to keep the root-squared sum of the contributions with different multiplicities below some limit in analogy with the Maréchal criterion in light optics [11]. Alternatively, one could use the root-mean-square (rms) residual phase shift instead of the maximum norm to adjust an optimum compensation scheme. This would result in slightly different AFI limits.

Since for a C_c/C_s-corrector the intrinsic and parasitic fifth-order axial aberrations dominate and need compensation, we ignore the intrinsic seventh-order axial aberrations which are typically small (5–20 mm). They do not even significantly modify the compensation schemes for the fifth-order aberrations.

Fig. 1 depicts the tolerable residual phase shift across the aperture for the even multiplicities $\nu = 0, 2, 4, 6$ after optimum compensation of the fifth-order aberrations according to the maximum norm. For phase contrast (PC) at 200 keV with an information limit of 20 nm^{-1}, equivalent to a usable aperture of 50 mrad, a fifth-order spherical aberration coefficient of $|C_5| \sim 4.0$–5.0 mm is optimum to achieve good PC also for low spatial frequencies down to 4 nm^{-1} or about 10 mrad. For amplitude contrast (AC) the compensation scheme for C_5 must be changed. For the non-round aberrations identical rules apply for AC and PC.

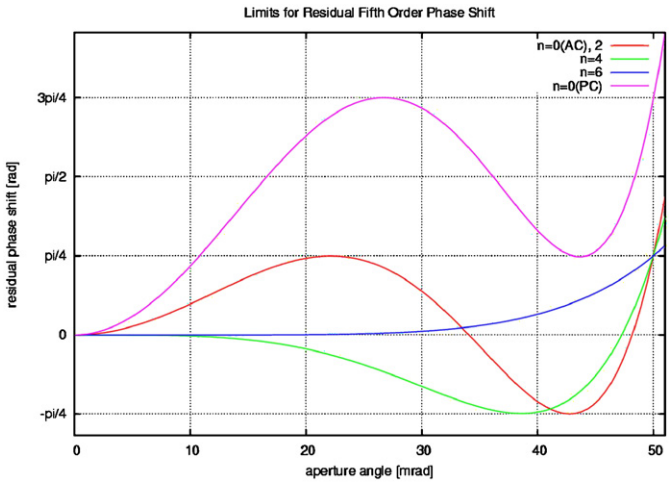

Fig. 1. Total phase shift caused by residual fifth-order aberration with multiplicity $n = 0, 2, 4, 6$ across the aperture for $\vartheta_{max} = 50$ mrad optimized for amplitude contrast (AC) and phase contrast (PC).

2.2. Off-axial aberrations

For CTEM applications the field of view is an important parameter and, hence, off-axial aberrations also have to be considered. At an off-axial image point additionally coma-type aberrations proportional to γ, the complex-valued off-axial position vector, contribute to the phase shift. For each odd multiplicity ν a certain distance $\gamma_\nu^{AFI} > 0$ can be defined such that the total residual phase shift is $|\Delta\Phi_\nu^{AFI}| \leqslant \pi/4$. For the spatial frequency g_{il} corresponding to the information limit this distance can be translated into a number of equally well-resolved image points N_ν^{AFI}. Again we consider each multiplicity separately. The total effect on the number of equally well-resolved image points can be estimated by the reciprocal root-squared sum of the individual contributions. For high-resolution imaging the number of equally well-resolved image points is an additional parameter to specify the quality of a certain instrument. Therefore, the strength of the intrinsic coma-type aberrations in third and fifth order is an important design criterion.

The proposed C_c/C_s-corrector will be designed for a high-resolution CTEM. Hence, the AFI criterion must be fulfilled not only at the center of the field of view but also for the full area of the specimen imaged onto the final screen or CCD camera. In order to exploit the capabilities of a $4k \times 4k$ camera at least 2000 equally well-resolved image points should be guaranteed, due to the necessary oversampling by at least a factor of 2. However, with a well-designed C_c/C_s-corrector 3000 image points per diameter can be achieved which is just sufficient for the next generation of CCD cameras which will have $8k \times 8k$ pixel.

Magnetic TEM objective lenses suffer from third-order azimuthal or anisotropic off-axial third-order coma. For a C_c/C_s-corrected CTEM with $g_{il} = 1/20\,\text{nm}$ at 200 keV this aberration would limit the number of equally well-resolved image points to less than 570 pixel.

For a single-gap objective lens the azimuthal coma is an unavoidable consequence of the Larmor rotation. Since double-gap objective lenses corrected for azimuthal coma with short focal length are not feasible for high beam energies due to the large magnetic field gradients, this aberration must be compensated by the C_c/C_s-corrector. Moreover, the corrector must not introduce other third-order coma-type aberration and the optical design must be optimized for minimum fifth-order coma-type aberrations.

2.3. Chromatic aberrations

The axial chromatic aberration is an incoherent aberration and, therefore, reduces the information limit of the instrument. The chromatic defocus induced by a change of energy is given by

$$\Delta C_1 = -C_c \cdot \Delta E/E_0.$$

Since the beam is not monochromatic, the contrast recorded in CTEM is effectively the incoherent average over a series of slightly defocused images. For a Gaussian energy spectrum of the electron gun with rms width $\sigma(E)$ the distribution of the chromatic focus spread is also Gaussian with

$$\sigma(C_1^{\text{chrom}}) = \frac{\sigma(E)}{E_0} C_c \tag{3}$$

and related to the full-width-half-maximum energy spread by $\Delta_{\text{FWHM}}E = \sqrt{8\ln 2}\cdot\sigma(E)$. The energy width usually accounts also for an additional broadening due to instabilities of the high-voltage supply.

We always refer to the relativistically corrected chromatic coefficient C_c, hence we use the chromatic parameter $\kappa = (E-E_0)/E_0$ with nominal energy E_0. In the literature some authors use other definitions and, therefore, require additional relativistic correction factors [12]. Care should be taken since the EM manufacturers usually state the smaller modified coefficient of chromatic aberration C_c* defined as

$$C_c^* = \frac{1+\varepsilon U_0}{1+2\varepsilon U_0} C_c$$
$$\text{with } \varepsilon = \frac{|e|}{2m_0c^2}. \tag{4}$$

The pre-factor amounts to, e.g. $f = 1.16$ for 200 kV and $f = 1.23$ for 300 kV. The easiest method to measure the chromatic coefficient C_c of the pre- or postfield of an objective lens is to change the high tension of the TEM without altering any lens currents and to measure the induced change of focus with respect to the specimen.

The chromatic focus spread reduces the information limit of a standard CTEM at 200 keV to typically $g_{il} = 8\,\text{nm}^{-1}$. For a CTEM equipped with C_c/C_s-corrector the information limit is not affected by the energy spread of the beam anymore. Even electrons which have suffered an energy loss in the specimen due to inelastic scattering do not blur the image contrast. EFTEM applications with a large energy window benefit very much from C_c-correction, since the usually very small chromatic parameter κ becomes larger by roughly one order of magnitude. Only for very large energy windows chromatic aberrations than the first-order, first-degree axial chromatic aberration C_c may gain importance.

For a CTEM equipped with C_c/C_s-corrector additionally the chromatic aberration of magnification must be considered. Although all lenses of the imaging system contribute to this off-axial chromatic aberration it can be avoided or at least kept very small by a careful design of the corrector and projector system.

Presently available aberration correctors for the CTEM correct for the spherical aberration only. These correctors cannot significantly improve the information limit or the number of equally well-resolved image points. The envisioned new state-of-the-art C_c/C_s-corrector must fulfill all of the above-mentioned criteria with respect to residual phase shift, field of view, and information limit. This type of aberration-corrected CTEM will have an—in terms of light optics—achromatic and aplanatic objective lens. In order to reflect the increased field of view by additionally correcting for the off-axial coma we prefer to call the novel aberration corrector as an *Achroplanat*.

3. Information limit

The image information transferred by an optical system is limited for high spatial frequencies by incoherent effects. This limitation can be quantified approximately by a damping-envelope function which accounts for the reduction of the observable contrast with increasing spatial frequency under the assumption that the object's scattering amplitude is that of a point scatterer (kinematic approximation, weak phase object).

This treatment refers to the instrumental information limit and neglects the influence of effects related to the specimen and the detector. For a given specimen the measured information limit will be equal to or lower than the instrumental information limit discussed here. Specimen properties which affect information transfer are the decrease of the atomic scattering amplitude for large scattering angles, inelastic or thermal-diffuse scattering, and beam-induced specimen damage.

The CTEM information limit is typically measured by the Young's-fringe method. When the results are compared with theoretical predictions it should be considered that the visible fringe contrast is not independent of the specimen. The influence of the atomic scattering amplitude and for thick or partially crystalline specimens dynamic scattering effects often makes a quantitative assessment difficult. To avoid an overestimation of the information limit it seems

preferable to select a specimen region which does not show Bragg spot in the diffractogram although—from a more practical point of view—the Bragg spots very conveniently document the magnification. Nevertheless, the Young's-fringe method is very well suited to compare the information limit from instrument to instrument with the same type of specimen.

In a well-designed and well-aligned standard microscope the instrumental information limit is mainly determined by

(1) the focus spread owing to the axial chromatic aberration C_c of the objective lens, the energy spread of the electron gun, and the stability of the high tension,
(2) the spherical aberration of the objective lens and the axial brightness $\beta_{200\,kV}$ of the electron gun (or the minimum feasible semi-convergence angle α_{sc} for a given illumination current density),
(3) the instability of the objective lens current, and
(4) the instability of the stage.

Compared to these strong contributions most other effects are negligible. For a system equipped with a C_c/C_s-corrector the dominant contributions (1) and (2) are eliminated and, therefore, a large number of additional minor effects become important and must be kept sufficiently small.

3.1. Image spread

A lateral time-dependent displacement of the image C_ε causes a loss of contrast for high spatial frequencies, if the change is not negligible during the exposure time. Image spread usually is anisotropic. For an instrument equipped with an Achroplanat the displacement can be caused by:

(1) mechanical vibrations of the stage in lateral direction,
(2) bending vibrations of the column,
(3) external AC stray fields such as high-frequency radio or micro waves,
(4) electrical instabilities of deflectors,
(5) electrical instabilities of lenses and multipole elements with off-axial alignment,
(6) dispersion caused by alignment deflectors and parasitic dipoles,
(7) dynamic equilibrium bulk effects of magnetic material and surface effects at electrodes and insulators.

The topics (1) and (2) depend on the mechanical stability, topic (3) on the electromagnetic shielding of the system. Topics (4) through (7) depend on the stability and required maximum strength of the power and voltage supplies and on the optical design and, in case (5), also on the optical alignment of the system (proper choice of rotation center and high-voltage center).

The influence of the image spread on the information limit can be quantified by an anisotropic spectral damping envelope function. Assuming a Gaussian (normal) distribution of the image spread C_ε with rms width $\sigma(C_\varepsilon)$ the envelope function for the xz- and yz-sections, respectively, has the following form:

$$K_{C_\varepsilon}(g) = \exp(-\tfrac{1}{2}(2\pi\sigma(C_\varepsilon))^2 g^2), \tag{5}$$

where $g = \omega/\lambda$ denotes the spatial frequency. The reduction of contrast for a certain maximum spatial frequency when increasing the image spread $\sigma(C_\varepsilon)$ is depicted in Fig. 2. The influence of the image spread depends only weakly on the shape of the disturbing signal. Also a uniform distribution or a sinusoidal perturbation cause a similar effect on the contrast as long as the strength of the perturbation is quantified in terms of rms.

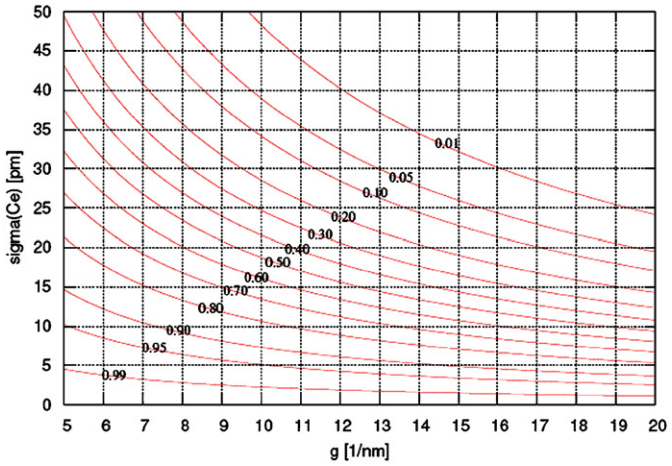

Fig. 2. Isolines of the contrast damping envelope function for normal distributed image spread with standard deviation $\sigma(C_\varepsilon)$ versus spatial frequency.

3.2. Focus spread

A change of the focusing strength in the xz- and/or yz-section causes a defocus C_1 and/or a two-fold astigmatism A_1. This round or two-fold focus spread leads to a loss of contrast for high spatial frequencies if the change is not negligible during the exposure time. For an instrument equipped with an Achroplanat the focus (or astigmatism) spread can be caused by:

(1) mechanical vibrations of the stage in z-direction,
(2) electrical instabilities of lenses and quadrupole elements.

Within the frame of validity of the linear contrast transfer theory the influence of the focal spread on the information limit can be quantified by a spectral damping envelope function. Assuming a Gaussian distribution of the focal spread with rms width $\sigma(C_1)$ the envelope function has the form

$$K_{C_1}(g) = \exp(-\tfrac{1}{2}(2\pi\lambda\sigma(C_1))^2 g^4), \tag{6}$$

where λ denotes the electron's wavelength and $g = \omega/\lambda$ is the spatial frequency. The isolines of equal contrast at

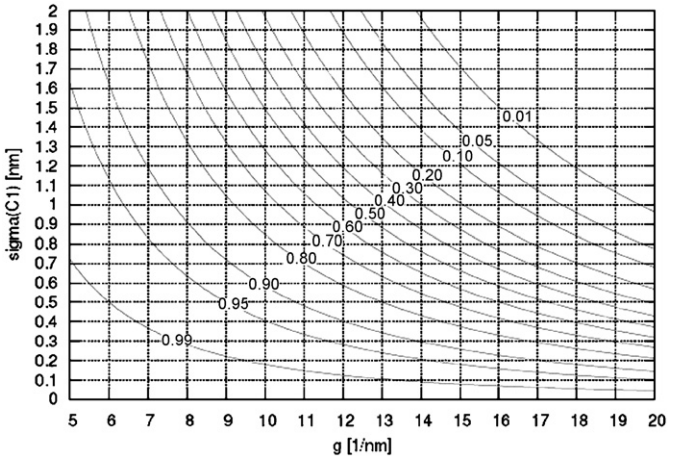

Fig. 3. Isolines of the contrast damping envelope function for normal distributed focus spread with standard deviation $\sigma(C_1)$ versus spatial frequency for a nominal beam energy of $E_0 = 200\,\mathrm{keV}$.

given focus spread $\sigma(C_1)$ versus scattering vector g are shown in Fig. 3. Again, the influence of the focus spread depends only weakly on the shape of the signal. Also a uniform distribution or sinusoidal perturbation causes a similar effect on the contrast as long as the perturbation is quantified in terms of rms.

3.3. Drift effects

Slowly changing time-dependent effects (typically below 0.1 Hz) that can be considered almost constant over the exposure time do not harm the information limit of the instrument but introduce drift. Strong drift effects render an instrument unusable for high-resolution microscopy since the optimally focused and aligned state is not sufficiently stable to observe real specimens. A microscope equipped with Achroplanat is eventually not more prone to drift effects than a standard instrument. However, since after the correction the available information limit is improved even small drift effects become apparent for the user. Therefore, the stability requirements for an ultrahigh-resolution TEM instrument with respect to drift will be more challenging than for a standard instrument.

For a system equipped with an Achroplanat image drift and focus drift can be caused by

(1) stage drift in lateral direction or in z-direction,
(2) drift of current and voltage supplies of dipoles or of, possibly off-axial, strongly focusing elements,
(3) thermal elongation caused by a change of the environmental or cooling water temperature or by a change of the internal power dissipation, and
(4) relaxation of magnetic material of the optical elements after a change of excitation.

All of the above topics must be considered and minimized during electro-mechanical design. Our aim is to keep image drift below 0.1 nm/min and focus drift below 0.5 nm/min.

4. Requirements for a CTEM with Achroplanat

4.1. Overall budgets

The information limit for a C_c/C_s-corrected instrument results from the cumulative effect of different incoherent perturbations. Therefore, we must define budgets for focus spread and image spread for the individual components of the system. We have decided to put slightly harder limits on the base instrument than on the corrector system, since the corrector has much more components and is more sensitive to high-frequency electronic noise. For the base system the influence of ΔE and α_{sc} can be neglected. If all components match their individual budgets, the total contrast damping for $g = 20\,\mathrm{nm}^{-1}$ at 200 kV will be a factor of 8 which would lead to a contrast transfer of 12.5%. This contrast of 12.5% seems not to be very high but is sufficient if all given budgets are not overspent. It is roughly equal to the common $1/e^2$-limit. The calculations are based on the upper noise limits in Table 2. For the calculation of the acceptable noise levels we assumed uncorrelated Gaussian noise.

4.2. Objective lens current stability

A fluctuation of the objective lens current results in a focal spread, according to the following relation:

$$\sigma(C_1) = F\sigma(I)/IC_c^* \quad \text{with } 1 \leqslant F \leqslant 2,$$

where C_c* denotes the modified coefficient of chromatic aberration of the objective lens. The pre-factor F is 1.0 for a strongly saturated lens. If the lens material is not strongly saturated—as it should be for a 300 kV objective lens operated at 200 kV—the worst case $F = 2.0$ applies. The upper frequency limit for AC noise seems to be in the 1 kHz range owing to the high impedance of the objective lens coil. In this frequency range the relative rms current stability for a typical TEM objective lens operated at 200 kV must be clearly better than 0.1 ppm to fulfill the requirements for an information limit of $g_{il} = 20\,\mathrm{nm}^{-1}$ according to Table 4.

4.3. Quadrupole stability for C_c-correction

C_c/C_s-correction by means of a quadrupole–octupole corrector is based on a modified Wien filter concept. In contrast to a classical Wien filter not electric–magnetic deflector elements, but electric–magnetic quadrupole elements are employed. Under ideal alignment these elements do not affect the course of the optic axis but focus or defocus the electron beam with respect to the xz- or yz-section, respectively. The superimposed electric and magnetic quadrupole fields are excited such that their

Table 2
Total budgets for the base instrument and the corrector

	Contrast transfer at information limit									
Base TEM, w/o ΔE and α_{sc}	50%									
Corrector	25%									
Both together	12.5%									
	Focus spread $\sigma(C_1)$ and image spread $\sigma(C_\varepsilon)$									
Acc. voltage U (kV)			80		120		200		300	
Wavelength λ (pm)			4.18		3.35		2.51		1.97	
Information limit g (nm^{-1})			12		20		20		20	
Max. acceptance angle α (mrad)			50		50		50		39	
	K_{C_1}	K_{C_ε}	$\sigma(C_1)$ (nm)	$\sigma(C_\varepsilon)$ (pm)	$\sigma(C_1)$ (nm)	$\sigma(C_\varepsilon)$ (pm)	$\sigma(C_1)$ (nm)	$\sigma(C_\varepsilon)$ (pm)	$\sigma(C_1)$ (nm)	$\sigma(C_\varepsilon)$ (pm)
Base instrument	70%	70%	0.45	11.2	0.36	8.9	0.27	6.7	0.34	6.7
Corrector	50%	50%	0.62	15.7	0.49	12.5	0.37	9.4	0.47	9.4
Both together	35%	35%	0.77	19.2	0.61	15.3	0.46	11.5	0.59	11.5

The standard deviation (rms) values are given for the focus spread and for the image spread allowable for both major components.

Table 3
Feasible relative mechanical precision requirements (element-to-element) and the typical resulting total axis misalignments between first and last elements of the corrector

	$\lvert\delta i\rvert$ (μm)	$\sigma(\Theta i)$ (mrad)	$\sigma(\omega)$ (mrad)	$\sigma(d)$ (μm)
Relative precision	14	0.1	0.2	20
Typical total	200	0.4	0.8	20

Table 4
Stability requirements (rms) imposed on the electronics supplies of the electric and magnetic quadrupoles of the principal correction units, for the other focusing elements and for the objective lens in parts-per-billion (ppb) to achieve an information limit of 20 nm^{-1} at 200 kV

Obj. lens type	High resolution	Ultrahigh resolution
Gap (mm)	5.4	2.0–3.0
Focal length (mm)	2.0	1.8
C_c (mm)	1.7	1.3
C_c* (mm)	1.45	1.08
C_3 (mm)	1.3	0.5
B_{3s} [1]	0.7	0.6
Principal corr. elements		
$\sigma(\Phi_{2c})/\lvert\Phi_{2c}\rvert$ (ppb)	40	54
$\sigma(\Psi_{2c})/\lvert\Psi_{2c}\rvert$ (ppb)	14.5	19.4
$r_{bore}\,\sigma(\Phi_1)$ (μV)	17.8	20.6
$\sigma(\Psi_1)$ (pT)	17.5	20.2
Other focusing elements		
$\sigma(I)/\lvert I\rvert$ (ppb)	447	598
Objective lens		
$\sigma(I)/\lvert I\rvert$ (ppb)	93	125

focusing strength is compensated for electrons with nominal energy. In addition strong adjustable chromatic aberrations are introduced: the chromatic defocus $C_{\alpha\kappa} = C_c$ and the chromatic two-fold astigmatism $C_{\tilde{\alpha}\kappa}$ The former of the two can be utilized to compensate for the chromatic aberration C_c of the objective lens, the latter has to be canceled. The correction requires an astigmatic path of rays or—in other words—a strongly two-fold shape of the beam within the principal correction elements.

This corrector principle has the inherent disadvantage that the strong fields required for correction compensate each other in Gaussian approximation but contribute strongly to the electrical stability budget of the system. To assess the stability requirements for C_c-correction we first concentrate on the quadrupole instabilities. Such instabilities are a direct consequence of the residual noise of the current and voltage supplies driving the correction elements.

A simple relation between the correction strength, the relative quadrupole stability of the correction elements, and the total focus spread exists. Here, we concentrate on the electrostatic quadrupole elements which are considered most critical owing to the large frequency range of electronic noise which has to be considered. Let $\sigma(\Phi_{2c})/|\Phi_{2c}|$ denote the relative standard deviation of the electric quadrupole instability, $\sigma(C_1^{QE})$ the standard deviation of the induced focus spread, C_c^{CORR} the required correction strength and the C_c^{EIGEN}/C_c^{CORR} feasible, minimum relative Eigen-C_c of the corrector, then we find

$$\frac{\sigma(\Phi_{2c})}{|\Phi_{2c}|} = \frac{1}{a}\frac{(\sigma C_1^{QE})}{C_c^{CORR}(1+(C_c^{EIGEN}/C_c^{CORR}))},$$
$$a = 2(1+\varepsilon\phi_0)(1+2\varepsilon\phi_0), \quad (7)$$

where $E_0 = e\Phi_0$ is the nominal beam energy and $\varepsilon = |e|/2m_0c^2 \sim 1/1.022\,\text{MeV}$. This relation illustrates that the

required stability of the critical corrector elements is determined by four independent factors:

(1) the acceptable focal spread $\sigma(C_1^{QE})$ for a given information limit,
(2) the relativistic factor $a \geqslant 2$ depending only on the acceleration voltage,
(3) the correction strength C_c^{CORR} required to compensate for C_c^{OL} of the objective lens, and
(4) the minimum relative eigen-C_c of the corrector C_c^{EIGEN}/C_c^{CORR}, which depends on the design of the corrector itself, on the feasible maximum electric field strength at the electric corrector elements, and on the minimum bore radius of the correction elements.

A similar relation also exists for the stability of the magnetic quadruples of the correction element. The magnetic quadrupoles also demand for very stable current drivers but the influence of higher-frequency electronic noise is rather weak owing to the impedance of the magnetic elements.

The relation (3) above assumes that the correction elements are driven by the minimum number of electrical supplies such that quadrupole instabilities introduce mainly defocus C_1 and not astigmatism A_1. This can always be achieved using symmetrically arranged pairs of correction elements driven by the same supplies. In this case the quadrupole instabilities caused by noise coming from the supplies are correlated with respect to each other. Using the smallest number of voltage supplies for the electric corrector elements is advantageous with respect to complexity and fault tolerance of the system. From the point of view of quadrupole stability requirements it could be worthwhile to consider a set of uncorrelated voltage supplies.

A system with more than one pair of correction elements can be arranged such that no (or only little) A_1-spread is generated and that the C_1-spread of the individual pairs of correction elements is statistically uncorrelated. This results in a sub-linear superposition of the noise contributions. In the ideal case of n corrector sub-units of equal strength with uncorrelated Gaussian noise $\sigma(C_1)$ the total focus spread is $\sqrt{n}\sigma(C_1)$, while the correction strength adds up linearly. It is not yet clear to what extent this theoretical improvement can be exploited in a practical system, since pick-up and cross-talk effects may act coherently on all sub-units of the corrector and make the noise more correlated than uncorrelated.

By setting $C_c^{EIGEN} = 0$ (what actually cannot be achieved for a feasible design), a fundamental limit for the minimum focal spread for a given quadrupole stability which only depends on the acceleration voltage and not on the actual design of the corrector can be derived from Eq. (7). It is important to note that this only accounts for the focus spread induced by the noise on the electric quadrupole element and neglects all other disturbances. In the non-relativistic limit $a = 2$ for small acceleration voltages the

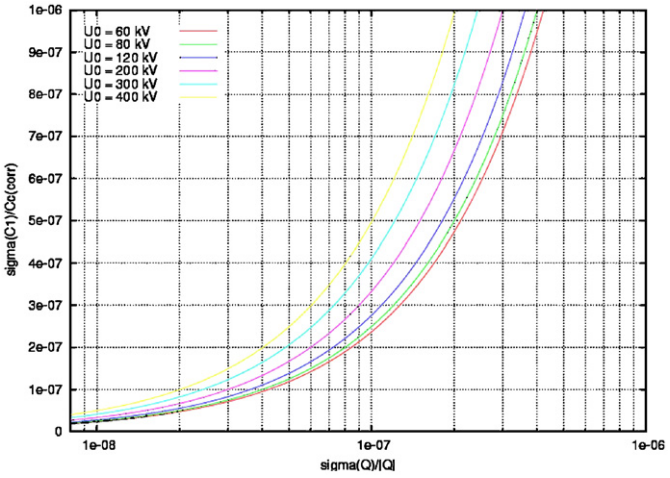

Fig. 4. Lower bounds for induced focus spread in units of C_c to be corrected versus relative electric quadrupole stability for different acceleration voltages ($C_c^{EIGEN} = 0$). We assume a corrector system driven by the minimum number of one bipolar supply and a negligible astigmatism spread. The cumulative effect of the electric and magnetic elements is not considered.

first-order Wien filter acts most effectively, for ultra-relativistic energies a is unbounded and the C_c-correction becomes ineffective. E.g. the dimensionless factor increases from $a = 3.33$ to 4.11 if we go from 200 to 300 kV, as it is depicted in Fig. 4. Simultaneously, we must allow for an increased C_c^{EIGEN} at 300 kV since the maximum feasible electric field strength for the electric quadrupole element is already reached at 200 kV and the correction strength must be adapted by a change of the magnification between the objective lens and the corrector.

For the new Achroplanat design for 200 kV a minimum relative eigen-C_c in the range of

$$0.4 \leqslant \frac{C_c^{EIGEN}}{C_c^{CORR}} \leqslant 0.6 \tag{8}$$

is achievable. This ratio is determined by the technologically feasible maximum electric field strength, the influence of dipole instabilities, and by higher-order axial and off-axial aberrations. For C_c-correction at 300 kV eventually a less favorable ratio must be accepted.

The achievable minimum induced focal spread increases with the required correction strength for a given relative quadrupole stability. Since the required correction strength equals the chromatic aberration of the objective lens this condition is not a problem for large-gap lenses or Lorentz microscopy because the acceptable total focus spread increases quadratically with the inverse target information limit. Nevertheless, for high-resolution imaging with an Achroplanat with maximum information limit, it is advantageous to keep the chromatic aberration C_c^{OL} of

the objective lens and of the transfer system as small as possible.

4.4. Optical alignment

In any practical charged particle optics system aberration assessment must account for aberrations caused by misalignments, manufacturing tolerances, and the inhomogeneity or remanence of the magnetic material. These aberrations are called parasitic aberrations. It is mandatory to compensate for the parasitic aberrations by means of alignment elements, typically deflectors and multipole stigmators. Without these alignment elements the tolerance requirements for any of the present aberration-correcting devices including the Achroplanat would be completely infeasible.

The Achroplanat will provide means to compensate for all relevant parasitic aberrations. We call these methods alignment tools (ATs). The concept of is a kind of abstraction. The ATs define recipes (most often linear combinations) how to operate the electric alignment elements, to achieve a desired optical effect. Every AT compensates for one or a small set of parasitic aberrations. It assumes that the alignment of the optical system is not too far away from the well-corrected state. It optimally operates within the linear regime and must be applied iteratively to compensate for larger amounts of parasitic aberrations. The parasitic aberrations remaining after optimum alignment are called the residual parasitic aberrations. One of the most important tasks in corrector design is to find a complete and efficient (e.g. almost orthogonal) set of ATs optimized for small higher-order residual parasitic aberrations.

For both, the definition and software control of the ATs theoretical methods originally developed for the C_s-corrector can be reused. Even before the first prototype is build we are able to analyze the feasibility of the corrector alignment by extended simulations. For a given design of the corrector and a well-defined set of ATs a large random set of geometrically disturbed model correctors has been simulated. The considered misalignments of consecutive optical elements are illustrated in Fig. 5. The intrinsic and parasitic aberrations can be calculated approximately by perturbation theory before and after the ATs have been applied. The final amount of residual parasitic aberrations and the excitation of the alignment elements found by the simulation can be analyzed statistically. This allows us to estimate the feasibility of the alignment and to derive the upper limits for the maximum allowed mechanical tolerances given in Table 3. The average and maximum excitation of an alignment element found in the simulation serves as a reliable guideline for the dimensioning of the individual elements.

Since drift effects are unavoidable even for the Achroplanat, as well as for any other aberration corrector, it is required to measure the residual aberrations periodically during operation. Our experience with the present TEM C_s-correctors shows that higher-order aberrations are very stable and realignment on a daily basis should be sufficient while second-order aberrations like axial coma B_2 and three-fold astigmatism A_2 require more frequent realignment, typically once every 2 or 3 h. The first-order aberrations defocus C_1 and two-fold astigmatism A_1 must be checked at least after a change of the object position and, if necessary, realigned.

5. Electronics design

The stability requirements imposed by the C_c/C_s-corrector are very demanding. The principal correction elements require a small number of highly stabilized unipolar current supplies (at least one) and unipolar high-voltage supplies (at least two). Additionally, the corrector system demands for a large number (more than 150) of additional unipolar or bipolar power supplies with reduced stability requirements.

5.1. Standard current driver

The standard current supplies will drive all multipole elements, except for the crossed electric/magnetic quadrupoles for C_c-correction. Nevertheless the noise contributions of a large number of elements act together, only reduced stability requirements must be fulfilled. A relative rms stability of $\sigma(I)/I \leqslant 4 \times 10^{-7}$ ($= 0.4$ ppm) is sufficient and can be realized by an electronics design based on the supplies also used for the present C_s-correctors. Only the power cabinet including digital control and cooling must be enhanced in order to host and address a considerably larger number of drivers.

5.2. Ultra-stable current driver

The ultra-stable power supplies will drive the magnetic quadrupoles of the principal correction element for C_c-correction. This pair of quadrupoles is excited by one current with the windings distributed symmetrically over the ferro-magnetic pole pins of a magnetic dodecapole element. The quadrupole has a fixed orientation. Therefore, the power supply is unipolar. The rms noise level with respect to the relevant frequency range should be in the range of $\sigma(I) = \Delta I/|I| \leqslant 1.5 \times 10^{-8} = 15$ ppb. Hence, the noise level should be a factor of 26 lower than for the stable current drivers.

The relative stability is determined by the allowed defocus/astigmatism spread according to the budgets defined in Table 2. The defocus/astigmatism should be stable over the time of a single image acquisition ($\leqslant 10$ s). For higher frequencies the noise is strongly damped by the inductance of the coils equipped with ferro–magnetic core.

The feasibility and the performance at the low and up to 10 kHz frequency range have been investigated by setting-up a state-of-the-art ultra-stable current driver. With this

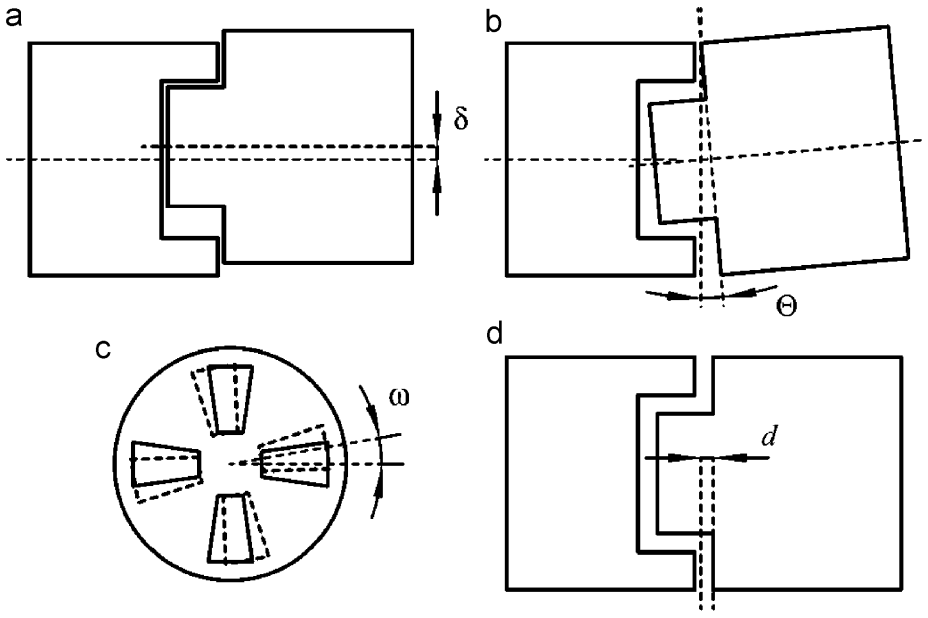

Fig. 5. Possible misalignments between consecutive elements. (a) The complex transversal shift $\delta = \delta x + i\delta y$ is assumed to have an upper bound $|\delta|$ given by the fitting adapter and to be equally distributed within this bound. (b) The complex tilt $\Theta = \Theta x + i\Theta y$ is assumed to be normal distributed in both components around zero with a given standard deviation $\sigma(\Theta i)$. (c) The rotation ω is assumed to be normal distributed around zero with a given standard deviation $\sigma(\omega)$. (d) The axial shift d is assumed to be normal distributed around zero with a given standard deviation $\sigma(d)$.

current driver it is the first time possible to demonstrate the feasibility of such a stable current supply and the results of the measurements can be seen in Fig. 6. The current driver is designed for an output current adjustable up to 1.25 A. Stability measurements have been performed. The analyzed signal shows the AC portion of the voltage signal across the sense resistor at 985 mA DC output current. Internally this signal is AC coupled (high-pass filter) and amplified using a low-noise Op-Amp, externally this signal is frequency limited (band-pass filter) and amplified using an SRS560 lab amplifier.

The oscilloscope screen prints show the output voltage of the on-board feedback amplifier (C3: blue). This trace is shown for control purposes only. C4 (green): The output voltage of on-board measuring amplifier (C4: green). The mathematical function C3–C4 (F1: orange). This trace is again shown for control purposes only. The parameter *P*6 is the peak-to-peak value of C4, parameter *P*8 is the rms value of C4. With respect to sense voltage 20 nV equals $10^{-9} = 1$ ppb relative stability.

5.3. Ultra-stable high-voltage supplies

The ultra-stable high-voltage supplies will drive the electric quadrupoles of the principal correction element for C_c-correction. The quadrupole has a fixed orientation. Therefore, it can be excited such that the electrodes with equivalent electric potential are electrically hard-connected. The rms noise level with respect to the relevant frequency range should be in the range of $\sigma(U) = \Delta U/|U| \leqslant 4 \times 10^{-8} = 40$ ppb.

The relative stability is determined by the allowed defocus/astigmatism spread according to the budgets defined in Table 2. The defocus/astigmatism should be stable over the time of a single image acquisition (<10 s). The upper limit is roughly given by the time of flight $T \leqslant 0.2$ ns of an electron through the multipole element ($v \sim 230$ mm/ns at 300 kV).

The control voltage can be derived from an ultra-stable, ultra-low-noise reference circuitry. Active control ranges from DC to about 10 kHz, higher frequencies can be filtered out passively. The stability of this ultra-stable voltage supply was measured on a prototype consisting of two channels. The output voltage is adjustable up to 5 kV and the stability measurements have been performed for 1 kV DC output voltage. The analyzed signal shows the AC portion of the voltage signal across the HV voltage divider. Internally this signal is divided, AC coupled (high-pass filter) and amplified using a low-noise Op-Amp, externally this signal is frequency limited (band-pass filter) and amplified using an SRS560 lab amplifier. The measured stability of the ultra-stable voltage supply can be seen in Fig. 7. Oscilloscope screen prints for frequency range 100 Hz to 30 kHz with 100 Hz/Div for ultra-stable voltage supply. The oscilloscope screen prints show the output voltage of on-board measuring amplifier (C4: bright green), the reference measurement with lab amplifier input grounded (M2: dark red), the FFT average of C4 (F4: pale green), and the FFT average of M2 (M4: steel blue). Parameter *P*8 is the rms value of C4. With respect to the output voltage 1 μV equals $10^{-9} = 1$ ppb relative stability.

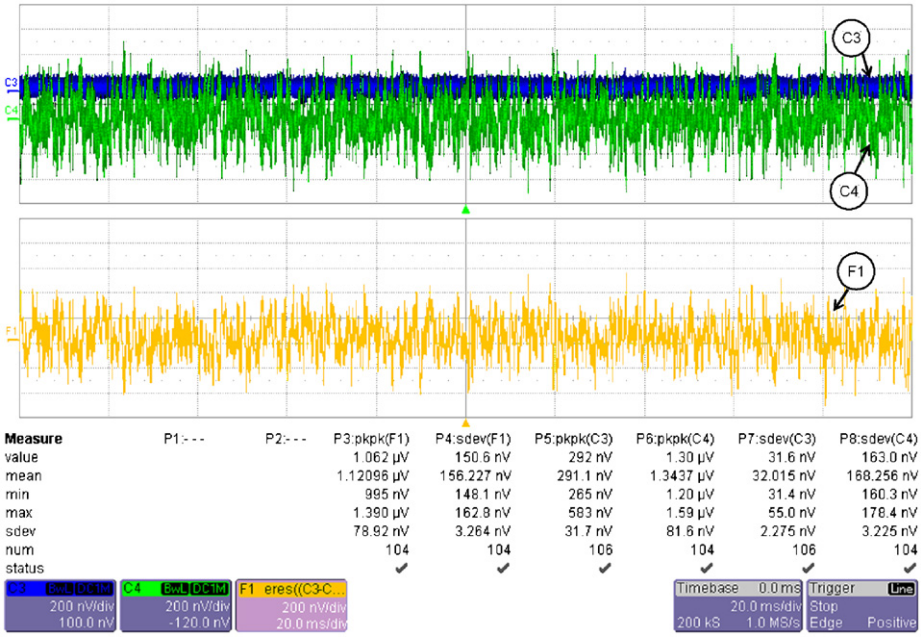

Fig. 6. Oscilloscope screen prints for frequency range 10 Hz to 1 kHz for ultra-stable current driver. The oscilloscope screen prints show the output voltage of the on-board feedback amplifier (C3: blue). This trace is shown for control purposes only. C4 (green): The output voltage of on-board measuring amplifier (C4: green). The mathematical function C3–C4 (F1: orange). This trace is again shown for control purposes only. The parameter $P6$ is the peak-to-peak value of C4, parameter $P8$ is the rms value of C4. With respect to sense voltage 20 nV equals $10^{-9} = 1$ ppb relative stability.

6. Conclusion

The envisioned C_c/C_s-corrected CTEM will not be restricted to just one field of application—ultrahigh resolution. On the contrary, it will offer a rather large variety of different possibilities, also for other acceleration voltages than the optimum voltage of 200 kV. However, the design of the Achroplanat has to be reviewed and where appropriate optimized for other applications because various objective lenses with considerably different optical parameters will be used. For in situ application, for example, a much larger focal length is mandatory. For biological applications a very large field of view might be more important than ultimate resolving power and, again, other criteria might be useful for EFTEM applications or for Lorentz microscopy. The present design of the Achroplanat is optimized for ultrahigh resolution and a resolving power of 50 pm is the goal. This ambitious goal imposes the strictest requirements for the base instrument and the Achroplanat among all alternative applications. Hence, the success of this ultrahigh-resolution CTEM will simultaneously demonstrate the feasibility of other C_c/C_s-correctors optimized with respect to different aspects.

The AFI criteria for acceleration voltages other than 200 kV follow physical scaling rules, such that the information limit in terms of a maximum aperture angle $\alpha_{il} = 50$ mrad is constant for $U \leqslant 200$ kV and in terms of the maximum spatial frequency $g_{il} = 20\,\mathrm{nm}^{-1}$ is constant for $U \geqslant 200$ kV. For the excitation of the electric quadrupoles we assume a maximum high voltage of about 4.5 kV even for $U \geqslant 200$ kV. For acceleration voltages below 200 kV the quadrupole excitation can be reduced.

From the budgets stated in Table 2 for the base instrument and the corrector, one can expect a considerable gain in the information limit owing to C_c-correction compared to C_s-only correction (lateral incoherence does not damp, C_c uncorrected and slightly increased by the corrector) as illustrated in Fig. 8. The relative stability requirements are less critical for smaller acceleration voltages. This is due to the fact that C_c-correction by crossed electric–magnetic quadrupoles is more effective for lower energies due to relativity and that the admissible defocus spread increases for constant aperture but increasing wavelength. For the idealized corrector system the AFI criteria can be fulfilled over the complete range of beam energies. The number of equally well-resolved image points might be slightly reduced for 120 and 80 kV. Our investigations have revealed that the lowest risk for achieving 0.05 nm AFI will be at an acceleration voltage of 200 kV. The comparison of the expected performance for different objective lenses shows that a 300 kV lens with standard gap is most critical. The optimum corrector performance for the goal of $g = 20\,\mathrm{nm}^{-1}$ could be achieved with a dedicated ultrahigh-resolution column and objective lens optimized for operation at 200 kV. In general C_c-correction is most attractive for low and medium beam energies. Compared to C_s-only correction the expected gain with respect to information limit is about 100% at 80 kV, 80% at 200 kV, and 50% at 300 kV if the CTEM is equipped with an Achroplanat.

With respect to the design of the ultra-stable electronics supplies for the corrector the critical components have been

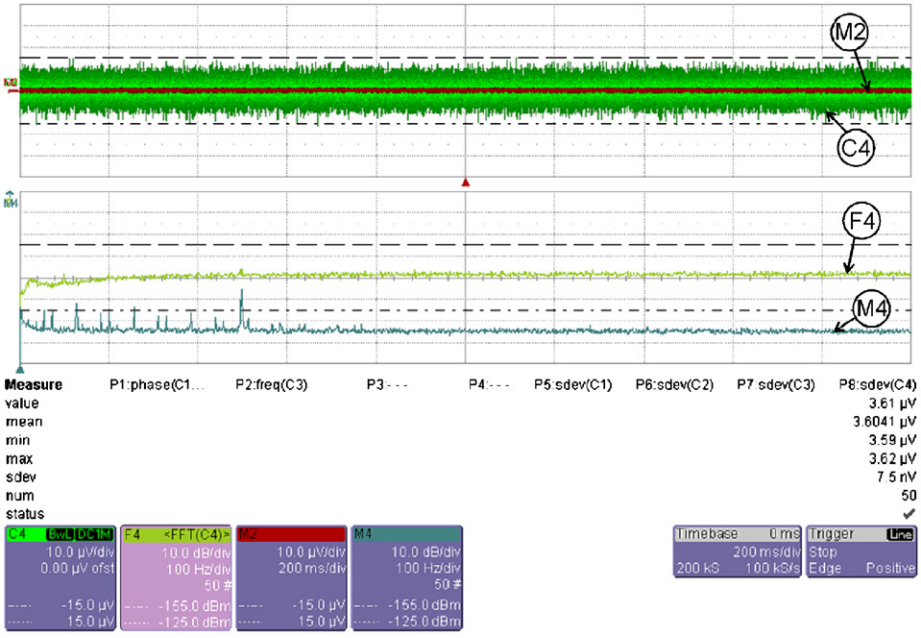

Fig. 7. Oscilloscope screen prints for frequency range 100 Hz to 30 kHz with 100 Hz/Div for ultra-stable voltage supply. The oscilloscope screen prints show the output voltage of on-board measuring amplifier (C4: bright green), the reference measurement with lab amplifier input grounded (M2: dark red), the FFT average of C4 (F4: pale green), and the FFT average of M2 (M4: steel blue). Parameter $P8$ is the rms value of C4. With respect to the output voltage 1 µV equals $10^{-9} = 1$ ppb relative stability.

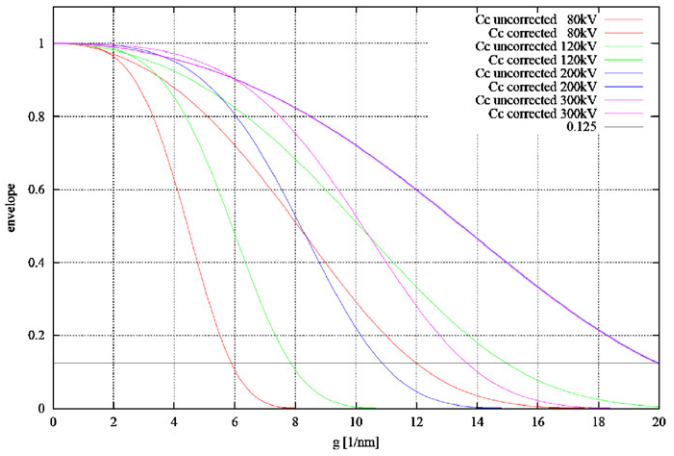

Fig. 8. Gain in information limit due to C_c correction for different primary energies. For the comparison we have chosen the 300 kV SuperTwin pole piece and its realistic C_c values for the different excitations. The lateral incoherence of the source is not included here since we assume the limiting case of an infinite brightness or at least C_s-correction.

identified. Based on a best-fit selection for these components, a principal design for the supplies has been investigated and tested. The encouraging results show the feasibility of the required stabilities at least in a laboratory environment. At lower energies the aperture becomes too big to be handled successfully by the corrector for this resolution limit.

On the basis of our theoretical and experimental investigations we are very much convinced that the Achroplanat combination with an appropriate base TEM will demonstrate so-called AFI up to and information limit of 20 nm^{-1} at 200 kV acceleration voltage. Although this sets challenging requirements for all components of the microscope, it seems to be feasible to fulfill them, using sophisticated but already existing technology and manufacturing techniques.

Acknowledgments

We gratefully acknowledge many valuable discussions with Bernd Kabius from Argonne National Laboratory over the last few years and continuing support and incentive by the TEAM community. This work was conducted as part of the TEAM project funded by the Department of Energy, Office of Science.

References

[1] O. Scherzer, Z. Phys. 101 (1936) 593.
[2] O. Scherzer, Optik 2 (1947) 593.
[3] J. Zach, M. Haider, Nucl. Inst. and Meth. Phy. Res. A 363 (1995) 316.
[4] D. Preizsas, H. Rose, J. Electron Microsc. 1 (1997) 1.
[5] H. Rose, Optik 84 (1990) 19.
[6] M. Haider, S. Uhlemann, E. Schwan, H. Rose, B. Kabius, K. Urban, Nature 392 (1998) 768.
[7] C.L. Jia, M. Lentzen, K. Urban, Science 299 (2003) 870.
[8] N. Tanaka, Proceeding of the ICM, vol. 16, Sapporo, 2006, 598.
[9] J.P. Morniroli, F. Houdellier, C. Roucau, J. Puiggalí, S. Gestí, A. Redjaïmia, Ultramicroscopy (2007), in press.
[10] H. Lichte, Ultramicroscopy 51 (1993) 15.
[11] M. Born, E. Wolf, Principles of Optics, Cambridge University Press, Cambridge, 1980, pp. 468–473.
[12] L. Reimer, Transmission Electron Microscopy, Springer, Berlin, 1984, p. 22 and 220.